Ceramics International 50 (2024) 33093–33097

Contents lists available at ScienceDirect

Ceramics International

journal homepage: www.elsevier.com/locate/ceramint

Short communication

Influence of the elemental composition on the structural and mechanical characteristics of entropy-stabilized HfZrCeYMgAlO thin films prepared by reactive magnetron sputtering

S. Zenkin [a,*], V. Bulakh [a], V. Uglov [b], A. Gaydaychuk [a], A. Mitulinsky [a], S. Linnik [a]

[a] Tomsk Polytechnic University, Tomsk, Russia
[b] Belarusian State University, Minsk, Belarus

ARTICLE INFO

Handling Editor: Dr P. Vincenzini

Keywords:
High entropy oxide
Magnetron sputtering
Mechanical properties
Entropy stabillization

ABSTRACT

Entropic stabilization of the crystal structure of solids was demonstrated for various systems, starting with metals and continuing with oxides, nitrides, borides, and more complex structures. The influence of additional thermodynamic driving forces sometimes allow to stabilize the material in a crystalline configuration that is unusual for it. In this paper, we focused on the HfZrCeYMgO system, which has shown excellent mechanical properties and a stable crystal structure. We added different concentrations of aluminum oxide, but found that even in significant quantities, it was embedded in the lattice without separating into separate phases. At the same time, we found that the addition of aluminum significantly increases the crystallinity of the coating as well as its mechanical characteristics. We associate the increase in coating crystallinity with a consistent increase in the entropy of mixing in the HfZrCeYMgAlO system.

1. Introduction

Entropic stabilization of the crystal structure of solids was demonstrated for various systems, starting with metals [1] and continuing with oxides [2], nitrides [3], borides [4], and more complex structures, for example, perovskites [5]. The influence of additional thermodynamic driving forces sometimes allow to stabilize the material in a crystalline configuration that is unusual for it [6]. Fixing a material in such a structure can lead to significant improvements in unusual characteristics, for example, the superionic conductivity of lithium demonstrated in the work [7]. Usually, high entropy (HE) alloys as well as high entropy ceramics demonstrate superior mechanical [8] and thermal [9] properties compared to traditional materials with a base of the same elements. This makes them a promising class of materials capable of wide application as protective and thermostable materials that increase the service life of turbines, jet engines, etc. [10]. Generally, synthesized high-entropy materials are characterized by a single crystal lattice and, accordingly, a crystalline microstructure [11]. However, there are a number of HE materials in which there is no crystalline structure [12]. At the same time, phase separation into individual saturated areas also does not occur [13]. Previously, we showed that a significant increase in the concentration of magnesium oxide in the HfZrCeYMgO system leads to its complete amorphization [14]. We assume that such an effect is caused by the growth of competing nanograins during the magnetron sputtering process, since magnesium oxide itself is not an amorphizing agent [15].

However, at equimolar concentrations, magnesium is incorporated into the crystal lattice without causing its disintegration into separate systems. This fact once again proves that the HfZrCeYO system is not only high-entropy but also entropy-stabilized. To confirm this statement, we synthesized HfZrCeYMgAlO films with the idea of introducing into the composition a material with a significantly different crystal lattice from the host oxide. Al_2O_3 under normal conditions has an $\bar{R}3c$ space group, Fig. 1a. Moreover, of the 6 oxides included in the high-entropy oxide HfZrCeYMgAlO, only cerium oxide, at normal conditions, has a fluorite structure, Fig. 1. Such a difference in crystal parameters requires additional conditions for stabilizing the crystal lattice. To achieve that, we used unbalanced magnetron sputtering for material preparation. The principle of metastable structure stabilization by magnetron sputtering is based on two non-equilibrium processes: the extremely fast heating of the system at the atomic level and the extremely fast cooling of the created material down to RT (less than 10 ps) [16]. This energy is delivered into a very small area of the growing material and dissipated in the close vicinity of every incident atom or

* Corresponding author.
E-mail address: zen@tpu.ru (S. Zenkin).

https://doi.org/10.1016/j.ceramint.2024.06.095
Received 11 April 2024; Received in revised form 28 May 2024; Accepted 7 June 2024
Available online 7 June 2024

ion. Such conditions make it possible to "freeze" a substance in a metastable state, which, together with the increased entropy of mixing, leads to the fixation of the material in a crystalline configuration that is unusual for it.

2. Materials and methods

HEO films were deposited on a monocrystalline Si (100). Before placing to the vacuum chamber samples were ultrasonically cleaned in acetone and isopropyl alcohol. High entropy oxide films were sputtered using two round unbalanced magnetrons equipped with HfZr (50/50 at. %) and CeY (33/66 at.%) targets. Mg and Al were added by the addition of small metal discs into the erosion zone of the magnetrons, Fig. 1b. The target diameter was 100 mm. The purity of the targets was 99.95 %. The magnetrons were powered by a pulsed DC power supply (1 kV, 5 kW, Applied Electronics, Russia). At the initial stage samples were cleaned by the Ar^+ ion source with an energy of 1.5 keV. The base pressure p_0 in the evacuated chamber was 8×10^{-4} Pa. The $HfZrCeYMgAlO_{2-\delta}$ films were deposited on substrate under the following conditions: discharge voltage $U_d = 300–350$ V, pulse frequency $f = 40$ kHz, substrate temperature $T_s =$ RT, substrate-to-target distance $d_{s-t} = 100$ mm, argon pressure $p_{Ar} = 0.5$ Pa and oxygen pressure $p_{O2} = 0.5$ Pa. Molar concentration in the growing films was controlled by the power ratio on the magnetron targets in the range of 0.5–2 kW.

The coatings surface, cross-sectional morphology, and elemental composition were studied using a transition electron microscope (TEM, JEM-2100 F, JEOL). The structural characteristics of the coatings were studied using an X-ray diffraction (Shimadzu XRD 6000) instrument with Cu Kα (λ = 0.154 nm) radiation. Sample curvature was measured by the optical profilometer (Micro Measure 3D Station, STIL) and film stress was calculated from the curvature measurements by using the Stoney formula. The research was carried out using the equipment of the CSU NMNT TPU, supported by the RF MES project 075-15-2021-710.

Using the X-ray diffraction method, the sizes of coherent scattering regions (CSR) (D) were determined from the broadening of the diffraction maxima. However, the width of the peaks is also affected by the magnitude of the microstresses ε, so there is a problem of separating the contributions from these two mechanisms to the final line width β. Typically, the Williamson-Hall method is used to separate contributions, which is based on the different dependences of two line broadening mechanisms on the X-ray diffraction angle θ:

$B_{CSR} = k\lambda/(D\cdot\cos\theta)$, $\beta_\varepsilon = 4\varepsilon\bullet\mathrm{tg}\theta$, here $k = \text{const} \approx 1$, form coefficient, λ - X-ray wavelength.

Moreover, the rule for taking into account the contributions of broadening depends on the shape of the diffraction line: Lorentz: $\beta = \beta_{CSR} + \beta_\varepsilon$, Gauss: $\beta^2 = \beta^2_{CSR} + \beta^2_\varepsilon$. In this case, the resulting grain size was averaged by the volume.

3. Results and discussion

As can be seen from the X-ray diffraction patterns, the coatings are single-phase systems based on a solid solution $(Hf,Zr,Ce,Y,Mg,Al)O_2$ with an FCC lattice (Fm-3m). The figure shows an absence of the preferential orientation for all compositions from $HfZrCeY_2O_9$ to $HfZrCe_2Y_4MgAl_2O_{18}$. As can be seen from Fig. 2b, the lattice parameter of the $(Hf,Zr,Ce,Y,Mg,Al)O_2$ solid solution is 0.52232–0.52393 nm. A change in the broadening of the diffraction peaks of the $(Hf,Zr,Ce,Y,Mg,Al)O_2$ solid solution was also detected for different samples. The results of calculating the CSR sizes, dislocation density, and microstrains obtained by the Williamson-Hall method in HfZrCeYMgAlO coatings are presented in Fig. 2 b,c,d.

As can be seen, with an increase in the number of components, the CSR size increases from 60 to 111 nm (the dislocation density decreases from $0.83*10^{11}$ cm^{-2} to $0.24*10^{11}$ cm^{-2}). At the same time, for the master oxide $HfZrCeY_2O_9$ this value is 28 nm (the dislocation density is $3.83*10^{11}$ cm^{-2}). Microdeformations in the coating increase from 0.4 to 1.3 % with an increasing number of system components. The results of determining macrostresses in HfZrCeYMgAlO coatings, obtained by the $\sin^2\Psi$ method for the (111) diffraction peak, are presented in Fig. 2d. Macrostresses are calculated for E = 200 GPa and $\nu = 0.298$. As can be seen from Fig. 2d, the stresses are compressive. The highest stress value (−6.95 GPa) corresponds to the $Hf_{2.3}Zr_{2.3}Ce_{2.3}Y_4MgAlO_{22}$ coating, and the lowest (−2.05 GPa) corresponds to the $HfZrCeY_2O_9$ coating. These stresses correlate with the film crystallinity, as described by TEM measurements.

Fig. 3 shows the results of transmission electron microscopy and selective electron diffraction for 3 characteristic compositions of the HfZrCeYMgAlO system. The initial four-component $HfZrCeY_2O_9$ system is characterized by a nanocrystalline structure. Moreover, the HRTEM results indicate a combination of randomly oriented nanocrystals, which is confirmed by the FFT results, in combination with areas with an amorphous structure, Fig. 3a. The measured value of the interplanar distance is 3.2 Å, which is consistent with the results of XRD analysis for a film of this composition. The transition to the 5-component $Hf_{2,3}Zr_{2,3}Ce_2Y_4MgO_{20}$ system is characterized by an increase in crystallite size, Fig. 3b. At the same time, HRTEM results show a decrease or complete absence of the amorphous phase. At the same time, the film still consists of randomly oriented nanocrystals without a pronounced

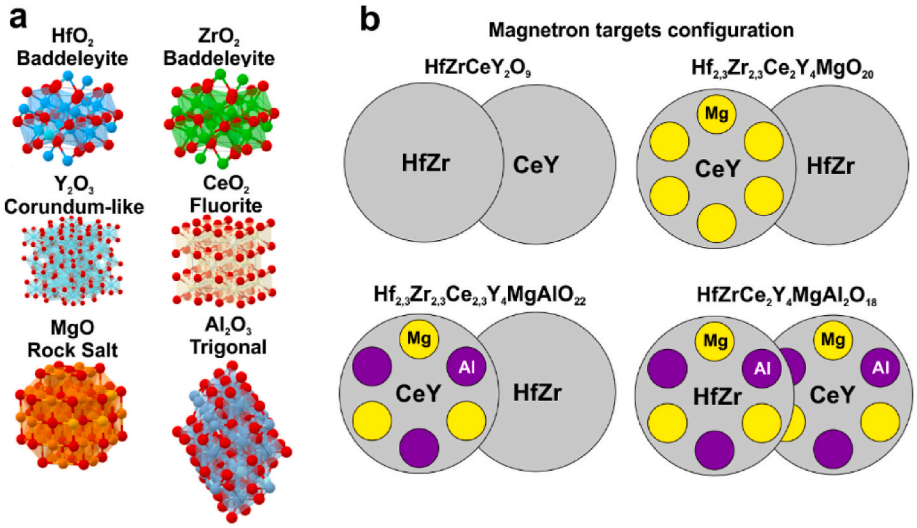

Fig. 1. Crystal structures of used oxides (a); magnetron target configuration for HfZrCeYMgAlO system deposition (b).

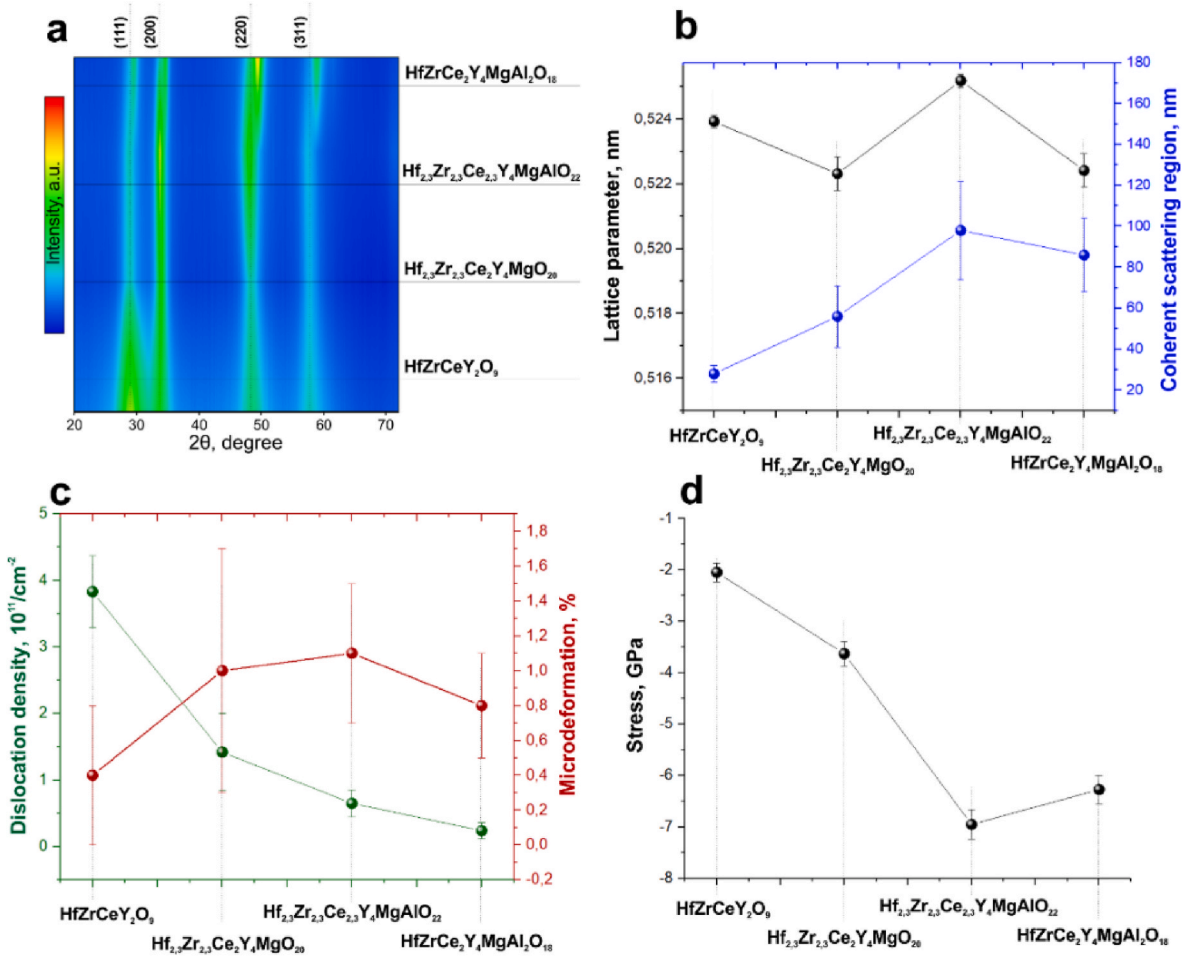

Fig. 2. XRD patterns (a); lattice parameter and coherent scattering region (b); dislocation density and microdeformation (c); and film stress(d) in dependence on the elemental composition of the film.

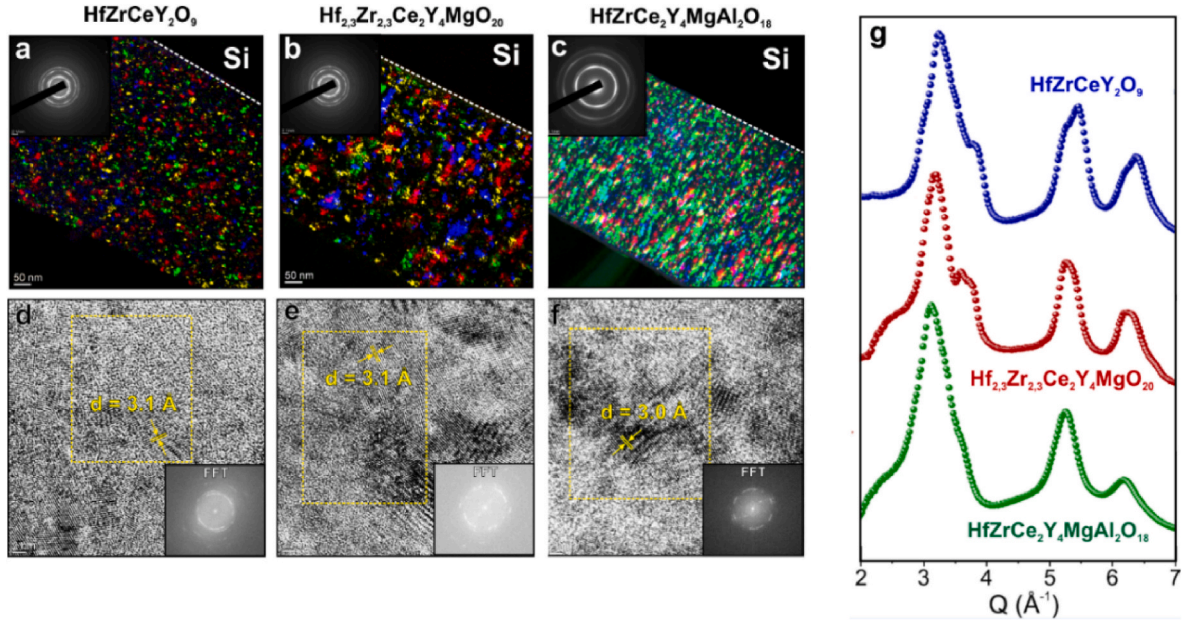

Fig. 3. False-colored TEM images and corresponding HRTEM of $HfZrCeY_2O_9$ (a,d) $Hf_{2,3}Zr_{2,3}Ce_2Y_4MgO_{20}$ (b,e) and $HfZrCe_2Y_4MgAl_2O_{18}$ (c,f), SAED intenscity profile (g).

dominant orientation, Fig. 3b. As in the case of the HfZrCeYO system, no separation or segregation of double and ternary oxides was detected, which is consistent with the results of XRD analysis. The measured value of the interplanar distance is 3.1 Å. Significant changes in the microstructure are characteristic of the $HfZrCe_2Y_4MgAl_2O_{18}$ system with an increased concentration of Al_2O_3, Fig. 3c.

The crystallinity of the coating increases sharply compared to 4- and 5-component compositions, Fig. 3f–and is correlated with the CSR value measured by XRD. At the same time, the coatings still remain nanocrystalline, with a grain size of less than 100 nm. The amorphous phase is completely absent, and the dominant structure begins to appear. The measured value of the interplanar distance is 3.0 Å. In this case, the film has a single crystal structure without additional phases. It can be assumed that the increased crystallinity is the result of the action of Al_2O_3, which is weakly correlated with the results from the literature [17]. Al_2O_3 is a strong amorphizing agent, and often forms amorphous coatings at magnetron sputtering deposition, and obtaining crystalline Al_2O_3 is a technological task that requires the use of special methods [18]. Thus, we argue that the increase in coating crystallinity is associated with a consistent increase in the entropy of mixing in the HfZrCeYMgAlO system.

For the HfZrCeYO system, from the point of view of the thermodynamics of high-entropy oxides, the addition of MgO and Al_2O_3 can be considered the inclusion of non-isostructural components in solid solutions, characterized by significant values of free transformation energies [19]. Previously, Chen et al. [20] showed that the system (Ce, Zr, Hf, Ti, Sn)O_2, which is similar in the master oxide composition, is entropy stabilized at an equimolar composition, and explained the stabilization of the structure by the configurational entropy achieved through several components. However, oxide solid solutions usually have a greater influence of ionic and covalent forces compared to metallic systems. These interactions depend on the crystalline and electronic structure of the material, which affect the mutual mixing of oxides. Therefor the mechanism of entropic stabilization can differ significantly from the mechanism for metals, where entropic stabilization is described by the influence of entropy and enthalpy factors. The transformation energy upon inclusion of non-isostructural components is significantly different for the components of the HfZrCeYMgAlO system. Thus, for the oxides ZrO_2, HfO_2, CeO_2, and Y_2O_3, it lies in the range of 8–10 kJ/mol, which ensures stabilization of the fluorite structure even for systems consisting of only two oxides, for example, ZrO_2– Y_2O_3 or HfO_2–Y_2O_3 [21], or the presence of a high degree of short-range order without a fixed long-range order in the CeO_2–Y_2O_3 system [22]. With the temperature rising in such systems, the entropy component ensures true ideal mixing and easily overcomes the endothermic enthalpy. The possibility of the formation of amorphous phases in such a system is significant in view of the fact that the transformation energy of monoclinic structure →amorphous structure and monoclinic structure →cubic structure for hafnium and zirconium oxides is almost the same [19]. As a result, the synthesized $HfZrCeY_2O_9$ composition largely contains an amorphous component. When adding MgO, which has a significantly higher free energy of transformation in the range of 35–40 kJ/mol, a violation of long-range order and a tendency to the formation of amorphous phases can be observed in the system, which is confirmed by the results of transmission microscopy for the composition $Hf_{2.3}Zr_{2.3}Ce_2Y_4MgO_{20}$. At the same time, the formation of double crystal structures other than fluorite in this system does not occur by analogy with the structures of $RE_2Zr_2O_7$ due to the order-disorder transition, which occurs in the range of 1700–2700 K depending on the ionic radius of the metal [23]. The equivalent temperature of atoms during deposition on the surface of a growing oxide film lies in the range of 1–5 eV, which at 1 eV = 11640 K significantly overlaps the transition temperature and ensures ideal mixing. The addition of Al_2O_3 with a transformation energy of 13 kJ/mol reduces the effect of MgO. One possible explanation for the increase in crystallinity of the HfZrCeYMgAlO system is that entropy-stabilized structures often exhibit a high degree of short-range order and it reduces the contribution of configurational entropy compared to ideal mixing due to the additional excess entropy [19]. This in turn leads to the fact that, at a certain stoichiometry of the oxide composition, long-range order eliminates configuration entropy, which leads to an increase in the symmetry of the initial disordered phase [19]. However, the studied oxide system is quite complex, and the mechanism of stabilization of crystal structures in it requires additional study.

The mechanical properties of the HfZrCeYMgAlO system are corelate realted to its composition. Fig. 4 shows the hardness of single or double oxides included in the HfZrCeYMgAlO system depending on the grain size, as described by the Hall-Petch effect. In addition, the same graph shows the hardness values of the studied compositions of the HfZrCeYMgAlO system. It can be seen that the hardness of HfZrCeYMgAlO coatings significantly exceeds the hardness of its constituent oxides with comparable grain sizes and ranges from 16,4 GPa for $HfZrCeY_2O_9$ to 20,1 GPa for $Hf_{2.3}Zr_{2.3}Ce_{2.3}Y_4MgAlO_{22}$. It is important to note, that films were deposited in a comparable magnetron sputtering process, Table 1, therefore their mechanical characteristics are determined by their elemental composition and corresponding structure.

Enhancement of the mechanical characteristics is probably primarily due to the stabilization of the cubic phases of ZrO_2, HfO_2 and Al_2O_3, which are the hardest modifications of these oxides [24]. In addition, an increase in the number of components leads to significant lattice deformations and an increase in the dislocation concentration, Fig. 2c. In addition, a positive effect on the hardness of the coating is a decrease in the amorphous component in the volume of the coating, which correlates with an increase in the number of components of the HfZrCeYMgAlO system, Fig. 3. At the same time, the hardness of the HfZrCeYMgAlO system, although slightly, increases with increasing Al_2O_3 concentration, which can be explained by the combined Hall-Petch effect and an increase in the concentration of the hardest aluminum oxide.

4. Conclusions

Based on the results of the study, the main conclusion can be drawn that the addition of aluminum oxide to the HfZrCeYMgAlO system increases its hardness by increasing the overall crystallinity of the coating and approaching the ideal grain size according to the Hall-Petch law. In this case, the system does not disintegrate into individual grains; the overall single crystal lattice is preserved. The addition of magnesium and aluminum to the master system reduces the dislocation density but,

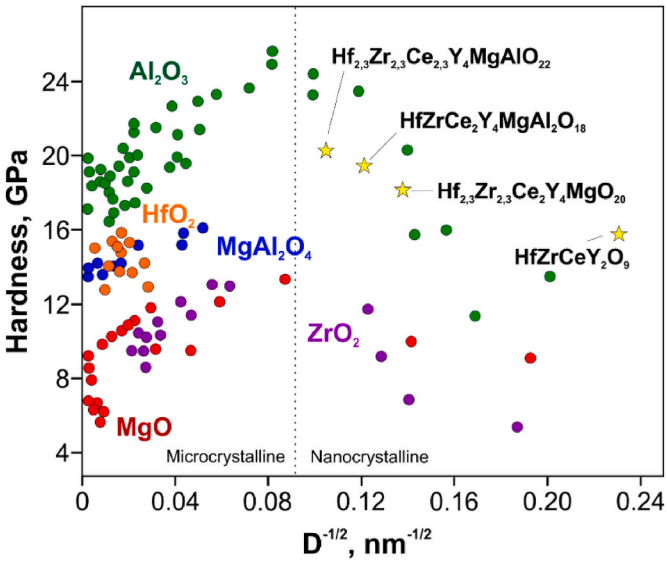

Fig. 4. Mechanical properties of studied high entropy films in comparison with traditional binary and thernary oxides.

Table 1
Elemental compositions and deposition parameters of studied high entropy films. Here U – substrate bias voltage, i_s – substrate current density, a_D – film deposition rate, ε_{bi} – energy delivered to the growing film, $\varepsilon_{bi} = U_s{*}i_s/a_D$, H – film hardness, E* - effective Young's modulus, W_e – elastic recovery.

Elemental Composition	*U* [V]	i_s [mA/cm^2]	a_D [nm/min]	ε_{bi} [MJ/cm^3]	*H* [GPa]	*E** [GPa]	W_e [%]	*H*/*E**
$HfZrCeY_2O_9$	−22	0,08	4,58	0,38	16,4	211	58	0,078
$Hf_{2,3}Zr_{2,3}Ce_2Y_4MgO_{20}$	−22	0,07	4,75	0,32	17,3	196	54	0,088
$Hf_{2,3}Zr_{2,3}Ce_{2,3}Y_4MgAlO_{22}$	−25	0,09	5,16	0,43	20,1	193	59	0,104
$HfZrCe_2Y_4MgAl_2O_{18}$	−23	0,08	4,86	0,38	19,6	210	57	0,093

at the same time, causes significant distortion of the crystal lattice up to 1.3 %. This distortion produces compressive stresses. The highest stress value (−6.95 GPa) corresponds to the $HfZrCe_2Y_4MgAl_2O_{18}$ coating, and the lowest (−2.05 GPa) corresponds to the $HfZrCeY_2O_9$ coating. The maximum hardness of the coating corresponds to the composition $Hf_{2.3}Zr_{2.3}Ce_{2.3}Y_4MgAlO_{22}$, which is close to equimolar. The results allow us to confirm that the system is not just high-entropy, but entropy-stabilized.

CRediT authorship contribution statement

S. Zenkin: Writing – original draft, Funding acquisition, Data curation, Conceptualization. **V. Bulakh:** Visualization, Validation, Investigation. **V. Uglov:** Methodology, Investigation. **A. Gaydaychuk:** Writing – review & editing, Investigation, Formal analysis. **A. Mitulinsky:** Writing – review & editing, Methodology, Investigation, Data curation. **S. Linnik:** Writing – review & editing, Validation, Supervision, Investigation, Data curation.

Declaration of competing interest

The authors declare that they have no known competing financial interests or personal relationships that could have appeared to influence the work reported in this paper.

Acknowledgement

This research was funded by the Russian Science Foundation, grant number 22-79-10069.

References

[1] J. Chen, X. Zhou, W. Wang, B. Liu, Y. Lv, W. Yang, D. Xu, Y. Liu, A review on fundamental of high entropy alloys with promising high–temperature properties, J. Alloys Compd. 760 (2018) 15–30.
[2] J. Gild, M. Samiee, J.L. Braun, T. Harrington, H. Vega, P.E. Hopkins, K. Vecchio, J. Luo, High-entropy fluorite oxides, J. Eur. Ceram. Soc. 38 (2018) 3578–3584.
[3] A.D. Pogrebnjak, B.A. Postolnyi, Y.A. Kravchenko, A.P. Shipilenko, O. Sobol, V. M. Beresnev, A.P. Kuzmenko, Structure and properties of (Zr-Ti-Cr-Nb)N multielement superhard coatings, J. Superhard Mater. 37 (2015) 101–111.
[4] Z. Zhang, S. Zhu, Y. Liu, L. Liu, Z. Ma, Phase structure, mechanical properties and thermal properties of high-entropy diboride (Hf0.25Zr0.25Ta0.25Sc0.25)B2, J. Eur. Ceram. 42 (2022) 5303–5313.
[5] M.C. Folgueras, Y. Jiang, J. Jin, P. Yang, High-entropy halide perovskite single crystals stabilized by mild chemistry, Nature 621 (2023) 282–288.
[6] C. Oses, C. Toher, S. Curtarolo, High-entropy ceramics, Nat. Rev. Mater. 5 (2020) 295–309.
[7] D. Bérardan, S. Franger, A.K. Meena, N. Dragoe, Room temperature lithium superionic conductivity in high entropy oxides, J. Mater. Chem. A 4 (2016) 9536–9541.
[8] H. Xiang, Y. Xing, F.-Z. Dai, H. Wang, L. Su, L. Miao, G. Zhang, Y. Wang, X. Qi, L. Yao, et al., High-entropy ceramics: present status, challenges, and a look forward, J. Adv. Ceram. 10 (2021) 385–441.
[9] Z. Li, J. Zheng, W. Zhang, Y. Zheng, W. Zhao, L. Xue, F. Yang, H.A. Chen, Promising high-entropy thermal barrier material with the formula ($Y_{0.2}$D $y_{0.2}Ho_{0.2}Er_{0.2}Yb_{0.2})_3Al_5O_{12}$, Materials 15 (2022) 8079.
[10] W.G. Fahrenholtz, G.E. Hilmas, Ultra-high temperature ceramics: materials for extreme environments, Scripta Mater. 129 (2017) 94–99.
[11] J. Chen, X. Zhou, W. Wang, B. Liu, Y. Lv, W. Yang, D. Xu, Y. Liu, A review on fundamental of high entropy alloys with promising high–temperature properties, J. Alloys Compd. 760 (2018) 15–30.
[12] W. Rong, Y. Chen, R. Dang, K. Huang, J. Xia, B. Zhang, J. Liu, H. Meng, Q. Cao, J. Wu, Amorphous high-entropy IrRuCrFeCoNiOx as efficient water splitting oxygen evolution reaction electrocatalysts, J. Alloys Compd. 971 (2024) 172786.
[13] S. Zenkin, A. Gaydaychuk, A. Mitulinsky, S. Linnik, Tailoring of optical, mechanical and surface properties of high-entropy Hf-Zr-Ce-Y-O ceramic thin films prepared by HiPIMS sputtering, Surf. Coat. Technol. 433 (2022) 128164.
[14] S. Zenkin, A. Gaydaychuk, A. Mitulinsky, V. Bulakh, S. Linnik, Effect of the MgO addition on the structure and physical properties of the high entropy HfZrCeYO fluorite ceramics, Coatings 13 (2023) 917.
[15] H. Yanagida, K. Koumoto, M. Miyayama, The Chemistry of Ceramics, John Wiley & Sons, Hoboken, NJ, USA, 1996, 0-471-95627-9.
[16] J. Musil, Š. Kos, S. Zenkin, Z. Čiperová, D. Javdošňák, R. Čerstvý, β-(Me1, Me2) and MeNx films deposited by magnetron sputtering: novel heterostructural alloy and compound films, Surf. Coating. Technol. 337 (2017) 75–81.
[17] J. Wang, Y.-H. Yu, S.C. Lee, Y.-W. Chung, Tribological and optical properties of crystalline and amorphous alumina thin films grown by low-temperature reactive magnetron sputter-deposition, Surf. Coating. Technol. 146–147 (2001) 189–194.
[18] J. Musil, J. Blažek, P. Zeman, Š. Prokšová, M. Šašek, R. Čerstvý, Thermal stability of alumina thin films containing γ-Al2O3 phase prepared by reactive magnetron sputtering, Appl. Surf. Sci. 257 (2010) 1058–1062.
[19] S.J. McCormack, A. Navrotsky, Thermodynamics of high entropy oxides, Acta Mater. 202 (2021) 1–21.
[20] K. Chen, X. Pei, L. Tang, H. Cheng, Z. Li, C. Li, X. Zhang, L. An, A five- component entropy-stabilized fluorite oxide, J. Eur. Ceram. Soc. 38 (2018) 4161–4164.
[21] T.A. Lee, A. Navrotsky, I. Molodetsky, Enthalpy of formation of cubic yttria-stabilized zirconia, J. Mater. Res. 18 (2003) 908–918.
[22] I.W. Chen, T.A. Lee, A. Navrotsky, Enthalpy of formation of yttria-doped ceria, J. Mater. Res. 20 (2005) 144–150.
[23] M.P. Saradhi, S.V. Ushakov, A. Navrotsky, Fluorite-pyrochlore transformation in Eu 2 Zr 2 O 7 —direct calorimetric measurement of phase transition, formation and surface enthalpies, RSC Adv. 2 (2012) 3328.
[24] G.C. Wood, T. Hodgkiess, The hardness of oxides at ambient temperatures, Mater. Corros. 23 (1972) 766–773.